Electrochemical advanced oxidation processes using novel electrode materials for mineralization and biodegradability enhancement of nanofiltration concentrate of landfill leachates

Marwa El Kateb, Clément Trellu, Alaa Darwich, Matthieu Rivallin, Mikhael Bechelany, Sakthivel Nagarajan, Stella Lacour, Nizar Bellakhal, Geoffroy Lesage, Marc Heran, et al.

Electrochemical advanced oxidation processes using novel electrode materials for mineralization and biodegradability enhancement of nanofiltration concentrate of landfill leachates.

Marwa El Kateb[1,2,4], Clément Trellu[1,3,*], Alaa Darwich[1], Matthieu Rivallin[1], Mikhael Bechelany[1], Sakthivel Nagarajan[1], Stella Lacour[1], Nizar Bellakhal[4], Geoffroy Lesage[1], Marc Héran[1], Marc Cretin[1,*]

[1] IEM, Univ Montpellier, CNRS, ENSCM, Montpellier, France

[2] Université de Tunis El Manar, Faculté des Sciences de Tunis, 2092 Tunis, Tunisie

[3] Laboratoire Géomatériaux et Environnement, LGE – Université Paris-Est, EA 4508, UPEM, 77454 Marne-la-Vallée, France

[4] Université de Carthage, Institut National des Sciences Appliquées et de Technologie, Laboratoire d'Echo-Chimie, 1080 Tunis, Tunisie

Manuscript submitted to Water Research for consideration

* Corresponding Author:

clement.trellu@u-pem.fr

+33 1 49 32 90 42

Graphical abstract

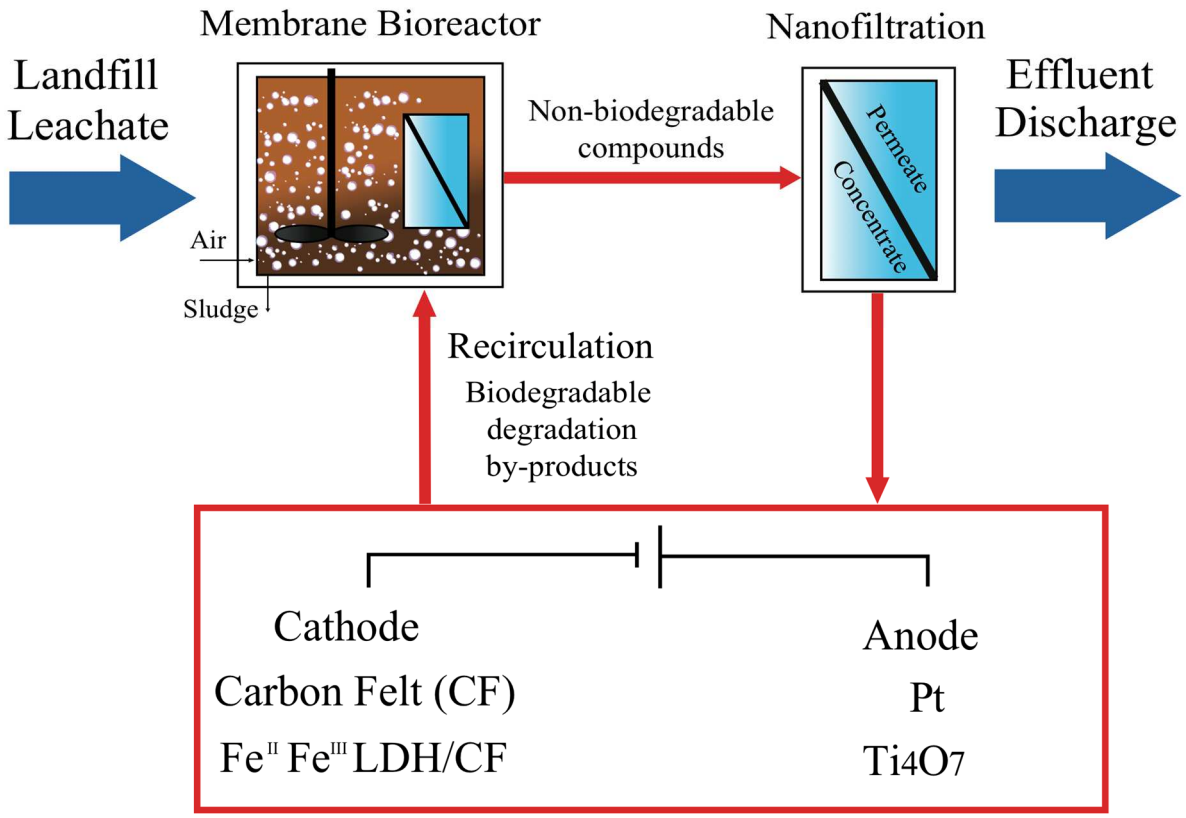

Electrochemical Advanced Oxidation Processes
Homogeneous/Heterogeneous electro-Fenton
Anodic Oxidation

Abstract

The objective of this study was to implement electrochemical advanced oxidation processes (EAOPs) for mineralization and biodegradability enhancement of nanofiltration (NF) concentrate from landfill leachate initially pre-treated in a membrane bioreactor (MBR). Raw carbon felt (CF) or $Fe^{II}Fe^{III}$ layered double hydroxides-modified CF were used for comparing the efficiency of homogeneous and heterogeneous electro-Fenton (EF), respectively. The highest mineralization rate was obtained by heterogeneous EF: 96% removal of dissolved organic carbon (DOC) was achieved after 8 h of electrolysis at circumneutral initial pH (pH_0 = 7.9) and at 8.3 mA cm^{-2}. However, the most efficient treatment strategy appeared to be heterogeneous EF at 4.2 mA cm^{-2} combined with anodic oxidation using Ti_4O_7 anode (energy consumption = 0.11 kWh g^{-1} of DOC removed). Respirometric analyses under similar conditions than in the real MBR emphasized the possibility to recirculate the NF retentate towards the MBR after partial mineralization by EAOPs in order to remove the residual biodegradable by-products and improve the global cost effectiveness of the process. Further analyses were also performed in order to better understand the fate of organic and inorganic species during the treatment, including acute toxicity tests (Microtox®), characterization of dissolved organic matter by three-dimensional fluorescence spectroscopy, evolution of inorganic ions (ClO_3^-, NH_4^+ and NO_3^-) and identification/quantification of degradation by-products such as carboxylic acids. The obtained results emphasized the interdependence between the MBR process and EAOPs in a combined treatment strategy. Improving the retention in the MBR of colloidal proteins would improve the effectiveness of EAOPs because such compounds were identified as the most refractory. Enhanced nitrification would be also required in the MBR because of the release of NH_4^+ from mineralization of refractory organic nitrogen during EAOPs.

25 # Keywords

26 Electro-Fenton; Anodic oxidation; Modified carbon felt; Sub-stoichiometric titanium oxide;

27 Landfill leachate; Biodegradability.

1. Introduction

Rainwater percolation through waste layers of landfills generates leachates containing a complex mixture of dissolved organic matter (DOM), inorganic compounds, heavy metals, and xenobiotic organic substances (Kjeldsen et al., 2002), which represents a significant hazard for the environment.

The implementation of a membrane bioreactor (MBR) followed by a nanofiltration (NF) step is one of the most efficient treatment strategy currently used for management of landfill leachates (Campagna et al., 2013; Amaral et al., 2016). However, NF is only a separation process. Biorefractory organic pollutants are accumulated and concentrated. Thus, the concentrate becomes an important residual issue for this treatment strategy (Van der Bruggen et al., 2003; Zhang et al., 2009, 2013). Landfill discharge of the concentrate is commonly performed. However, some national regulations do not allow such practice and it clearly does not fix the long-term issue. In recent years, several processes have been investigated and applied at industrial scale for the treatment of NF concentrate. For example, adsorption processes are effective to remove organic matters in NF concentrate, but they are strongly limited by the high organic charge of such effluents compared to the adsorption capacity of adsorbent materials. Besides, membrane distillation and evaporation processes are substantially limited by the high cost of equipment and energy consumption (Cui et al., 2018).

During the last two decades, electrochemical advanced oxidation processes (EAOPs) have received great attention for efficient degradation of a large range of hazardous and biorefractory organic compounds. They are based on *in situ* electrogeneration of hydroxyl radicals ($^{\bullet}OH$), a non-selective and powerful oxidizing agent ($E^{\circ}(^{\bullet}OH/H_2O)$ = 2.80 V *vs* SHE) (Brillas et al., 2009; Comninellis et al., 2008; Martínez-Huitle et al., 2015; Panizza and Cerisola, 2009). EAOPs provide also several technical advantages such as high versatility,

52 easy operation, possibility for automation and low consumption of chemical reagents
53 (Radjenovic and Sedlak, 2015; Sirés et al., 2014). However, complete mineralization of
54 organic compounds requires high energy consumption. Therefore, the combination of EAOPs
55 with biological processes is currently more and more investigated as a feasible option for
56 improving the global cost-effectiveness of the process (Oller et al., 2011; Ganzenko et al.,
57 2014, 2018; Trellu et al., 2016a; Olvera-Vargas et al., 2015). In order to achieve reliable
58 conclusions, the accurate assessment of biodegradability enhancement by EAOPs requires the
59 use of proper measurement tools such as respirometric methods (Reuschenbach et al., 2003).

60 Anodic oxidation (AO) and electro-Fenton (EF) are the most popularized EAOPs (Brillas et
61 al., 2009; Panizza and Cerisola, 2009; Martínez-Huitle et al., 2015; Oturan et al., 2015). AO is
62 based on the generation of hydroxyl radicals ($^{\bullet}OH$) via water oxidation at the surface of
63 anodes (M) with high overvoltage for oxygen evolution reaction (Eq. 1) (Panizza and
64 Cerisola, 2009; Trellu et al., 2017; Özcan et al., 2008), while $^{\bullet}OH$ are generated
65 homogeneously in the bulk during the EF process through the Fenton's reaction (Eq. 2)
66 (Brillas et al., 2009; Ma et al., 2016; Zhang et al., 2007). H_2O_2 and iron (II) are continuously
67 electrogenerated at the cathode by reduction of dissolved oxygen (Eq. 3) and iron (III)
68 reduction (Eq. 4), respectively. External oxygen supply is required and an iron source must be
69 either initially added at catalytic amount to the treated solution (homogeneous EF) or
70 embedded onto suitable electrode materials (heterogeneous EF).

71 $M + H_2O \longrightarrow M(^{\bullet}OH) + H^+ + e^-$ (Eq. 1)

72 $Fe^{2+} + H_2O_2 + H^+ \longrightarrow Fe^{3+} + {}^{\bullet}OH + H_2O$ (Eq. 2)

73 $O_{2(g)} + 2H^+ + 2e^- \longrightarrow H_2O_2$ (Eq. 3)

74 $Fe^{3+} + e^- \longrightarrow Fe^{2+}$ (Eq. 4)

Homogeneous EF requires external iron source and acidic pH (*i.e.* pH 2.5 – 3.5) that prevents iron precipitation (Brillas et al., 2009). Besides, heterogeneous EF using for example pyrite (Ammar et al., 2015) or iron loaded sepiolite (Iglesias et al., 2013) as iron source has been developed in order to operate the process over a wide pH range (Ganiyu et al., 2018; Poza-Nogueiras et al., 2018). Innovative electrodes have been also synthesized and studied as both heterogeneous catalyst source and cathode materials (Zhang et al., 2012; Wang et al., 2013; García-Rodríguez et al., 2016; Ganiyu et al., 2017a). Particularly, the modification of raw carbon felt (CF) with CoFe or $Fe^{II}Fe^{III}$-layered double hydroxide (LDH) also led to an increase of the electroactive surface area, which in turn improved the generation of H_2O_2 and the global efficiency of the heterogeneous EF process (Ganiyu et al., 2017a, 2018). However, to the best of our knowledge, none study focused on the application of such promising electrodes for the treatment of real wastewaters.

As regards to anode materials, sub-stoichiometric titanium oxides (especially Ti_4O_7) recently received great attention for application in wastewater treatment by AO (Guo et al., 2016; Ganiyu et al., 2016; Trellu et al., 2018b). Ti_4O_7 anode is able to generate large amounts of physisorbed hydroxyl radicals ($Ti_4O_7(^{\bullet}OH)$) for the degradation and mineralization of organic contaminants. Besides, this material has the potential to become a low-cost anode compared to the well known boron-doped diamond anode (Ganiyu et al., 2017b; Trellu et al., 2018b). However, to the best of our knowledge, such anode material has also still not been applied for the treatment of real effluents.

The objective of this study was to investigate the application of these novel electrode materials for the treatment of a NF concentrate of landfill leachate initially pre-treated in a MBR, which represents an important challenge for environmental engineering. Various configurations (*i.e.* homogeneous EF, heterogeneous EF, heterogeneous EF/AO) and operating conditions were studied. The efficiency for mineralization of organic compounds

was compared. A particular attention was also given to the understanding of mineralization mechanisms by using various analytical tools: (i) DOM was characterized by three-dimensional excitation and emission matrix fluorescence (3DEEM), (ii) degradation by-products such as short-chain carboxylic acids were identified and quantified by ion-exclusion HPLC, and (iii) inorganic ions released during the mineralization process were identified and quantified by ion chromatography. Moreover, acute toxicity of the effluent was assessed by Microtox® analysis and the possibility to use such EAOPs as a pre-treatment before recirculation towards the MBR was assessed by using respirometric method under similar conditions than in the real industrial MBR. Finally, recommendations were given by taking into consideration the interdependence of MBR process and EAOP in a combined treatment strategy.

2. Materials and methods

2.1 Chemicals

For the preparation of $Fe^{II}Fe^{III}$-LDH modified CF, iron III nitrate nonahydrate $Fe(NO_3)_3.9H_2O$ (CAS 7782-61-8, 98% purity), iron II sulfate heptahydrate $FeSO_4.7H_2O$ (CAS 7782-63-0, >99% purity), urea $CO(NH_2)_2$ (CAS 57-13-6) and ammonium fluoride NH_4F (CAS 12125-01-8, 99% purity) were supplied by Sigma Aldrich. Ultra-pure water (Millipore Mill-Q system, resistivity >18 MΩ.cm at 25 °C) was used for the preparation of all solutions.

2.2 Landfill leachate (NF concentrate)

The NF concentrate was collected from a landfill leachate wastewater treatment plant (WWTP) in the south of France. The raw landfill leachate was initially treated in a MBR, then

followed by a NF step. The concentrate from the NF step was collected and stored in a refrigerator at 4 °C.

2.3 Electrochemical setup and electrode materials

Experiments were conducted in an undivided cylindrical glass containing 220 mL of NF concentrate at room temperature (25 °C). The electrochemical cell was similar to the one used in several previous studies (Ganiyu et al., 2016; Trellu et al., 2016b). Either raw CF (for homogeneous EF) or $Fe^{II}Fe^{III}$-LDH modified CF (for heterogeneous EF) was employed as cathode (20 x 6 cm; 120 cm^2), positioned on the inner wall of the cylindrical cell. CF (99.0%, 6.35 mm thick) was provided by Alfa Aesar. $Fe^{II}Fe^{III}$-LDH modified CF was prepared by *in-situ* solvothermal process as reported elsewhere (Ganiyu et al., 2018). LDH coating was 0.62 ± 0.04 mg cm^{-2}, which was also in agreement with what has been reported previously (Ganiyu et al., 2018). For homogeneous EF experiments, 0.2 mM of Fe^{2+} was added to the solution and initial pH was adjusted at 3 (values usually reported as optimal). For heterogeneous EF experiments, none Fe^{2+} was externally added and pH was not initally adjusted.

The anode was either a 24 cm^2 (3 x 8 cm) platinum mesh (for homogeneous and heterogeneous EF) or a 32 cm^2 (4 x 8 cm) Ti_4O_7 thin film plasma deposited on Ti substrate (for heterogeneous EF/AO) from Saint-Gobain Research Provence, France. Ti_4O_7 powder used for plasma deposition was prepared by carbothermal reduction of TiO_2 as already reported by our group (Ganiyu et al., 2016, 2017b). These rectuganlar-shaped anodes were placed at the center of the cylindrical electrochemical cell, with an average interelectrode distance of 3 cm.

Electrodes were connected to a DC power supply (CNB Electronique) with applied current set at 1000 mA (j = 8.3 mA cm^{-2}, calcultated from the cathode surface, which is the working

147 electrode during the EF process) or 500 mA (j = 4.2 mA cm^{-2}). A magnetic stirrer was used to
148 improve mass transport of chemical species toward/from the electrodes. The solution was
149 saturated with O_2 by bubbling compressed air through a glass frit 10 min before starting the
150 experiments and all along the electrolysis. The conductivity of the NF concentrate was high
151 enough to ensure the electrolysis without any additional supporting electrolyte. For
152 comparison, a reference experiment was also carried out using raw carbon felt cathode, Pt
153 anode, without adding any source of iron and without initial pH adjustment.

154

155 **2.4 Dissolved organic carbon and chemical oxygen demand analysis**

156 Mineralization rate of NF concentrate was determined by total organic carbon (TOC) analyses
157 using the Shimadzu TOC-L analyzer based on the 680 °C combustion catalytic oxidation
158 method. All samples were filtrated through 0.45 µm regenerated cellulose (RC) membrane
159 filters. Therefore, results are reported as dissolved organic carbon (DOC).

160 Chemical oxygen demand (COD) was analyzed by the method AFNOR NFT 90-101 using
161 Hach COD kits.

162

163 **2.5 Respirometric method for the determination of biodegradability**

164 Biodegradability was assessed with a BM-T Advance Respirometer (SURCIS S.L, Spain),
165 which consists in a 1 L capacity vessel, provided with an oxygen probe (Hamilton) and
166 temperature control system. The activated sludge used in the bioassays was collected from the
167 aerated tank of the landfill leachate WWTP using MBR and was thus acclimatized to the
168 effluent. The samples were evaluated without pH adjustment because of the high buffer
169 capacity of the landfill leachate samples. Continuous aeration and agitation were applied to

ensure air saturation conditions. Temperature was maintained at 20 °C during the tests and the standardization with sodium acetate method was applied (conversion rate adjustment according to instructions given by the respirometer's manufacturer). In order to inhibit the nitrification process and measure the sample effect only on the heterotrophic bacteria, 1.5 mg $gVSS^{-1}$ of N-allylthiourea was added before the beginning of each trial.

For biodegradability assays, 700 mL of endogenous activated sludge and 300 mL of target sample were introduced in the respirometer. The biodegradability of samples pre-treated by EAOPs was assessed through R tests (Fig. SI 1). The ratio between biodegradable COD (bCOD) and DOC (bCOD/DOC) was used for determination of the biodegradable character of each sample. A biodegradability enhancement index (BE) was calculated by using Eq. 5.

$$BE = \frac{\left(\frac{bCOD_t}{DOC_t}\right)}{\left(\frac{bCOD_0}{DOC_0}\right)} \qquad \text{(Eq. 5)}$$

Where $bCOD_t$ and DOC_t are bCOD (in $gO_2\ L^{-1}$) and DOC (in $gC\ L^{-1}$) after t hours of treatment by EAOPs.

2.6 Characterization of dissolved organic matter by three-dimensional excitation and emission matrix fluorescence (3DEEM)

Natural organic matter was characterized by 3DEEM fluorescence using a Perkin-Elmer LS-55 spectrometer (USA). The dilution factor was 200 for all samples. The procedure reported by Jacquin et al. (2017) was used for fluorescence spectra acquisition and data extraction. Chen et al. (2003) divided fluorescence spectra into five different areas corresponding to different groups of fluorophores, *i.e.* regions I and II for aromatic proteins, region III for fulvic acid-like (FA-like) fluorophores, region IV for soluble microbial by-product-like (SMP-like) fluorophores and region V for humic acid-like (HA-like) fluorophores (Chen et

al., 2003). Similarly to the study of Jacquin et al. (2017), 3DEEM results were analyzed by taking into consideration only 3 different zones, *i.e.* zone I' for region I + II (aromatic proteins), zone II' for region IV (SMP-like) and zone III' for region III + V (HA + FA-like). Calculation of the volume of fluorescence in these different zones was achieved following the method from Jacquin et al. (2017).

The procedures for ICP-MS analysis, toxicity test (Microtox®), identification/quantification of inorganic ions and identification/quantification of short-chain carboxylic acids are provided in Supplementary Information (SI)

3. Results and Discussion

3.1 Characterization of the NF concentrate effluent

The characteristics of the NF concentrate are presented in SI (Table SI 1). The effluent was a dark brown liquid having a slightly alkaline pH and high organic charge. The conductivity (3.1 mS cm^{-1}) was between 3 and 10 times lower than values reported in the literature (10 – 33 $mS.cm^{-1}$) (Li et al., 2015; Hu et al., 2018; Xu et al., 2017). This might be ascribed to the high diversity of landfill leachate and to a lower retention of ionic species by the NF step. In fact, the concentration factor of divalent (Mg^{2+} and Ca^{2+}) and monovalent (Na^{+} and K^{+}) inorganic cations was only 3.1 ± 0.3 and 1.7 ± 0.2, respectively. Monovalent ions are less retained by the NF membrane because of lower charge interactions (Van der Bruggen et al., 2004). The COD content (2.1 gO_2 L^{-1}) of the NF concentrate was also in the low range of values usually reported in the literature (1.7 – 5.5 gO_2 L^{-1}) (Li et al., 2015; Hu et al., 2018; Xu

et al., 2017) because of (i) operation of the NF process with a lower concentration factor and/or (ii) lower initial organic loading rate of the effluent pre-treated by the MBR.

The ratio between bCOD and total COD or total DOC was low (bCOD/COD = 0.12 or bCOD/DOC = 0.26), thus indicating the low biodegradability of the concentrate owing to the presence of high-molecular weight and non-biodegradable compounds. A high concentration of nitrate ($[NO_3^-]$ = 90 mg L^{-1}) was observed due to the complete nitrification of NH_4^+ in the MBR and a partial denitrification in the anoxic tank. As regards to metals, Sr ion was the most concentrated (6.0 mg L^{-1}) and high concentrations of As (0.38 mg L^{-1}) and Cr (0.67 mg L^{-1}) ions were also reported. These metals are released by different wastes discarded in landfills such as glass products (Ponthieu et al., 2007), fluorescent lights and ceramics (Mahindrakar and Rathod, 2018). Besides, the high concentration of Sb (1.2 mg L^{-1}) indicates an important contamination from plastic decomposition (Westerhoff et al., 2008).

3.2 Mineralization efficiency by EAOPs

Various experiments were performed in order to evaluate the efficiency of different EAOPs (*i.e.* homogeneous EF, heterogeneous EF, heterogeneous EF/AO).

First, volatilization and adsorption phenomena were evidenced by bubbling oxygen into the electrochemical reactor without any current applied. Under these conditions, DOC content decreased and reached a plateau after 1 h with around 16±2% removal due to volatilization of volatile organic compounds and adsorption of hydrophobic compounds on CF. Besides, it was also observed that initial pH adjustment at 3 decreased the DOC value by 15±5% because of the precipitation of humic acids.

Second, experiments were carried out under constant current density applied to the electrodes. As shown in Fig. 1A, 96% of DOC removal was obtained after 8 h of electrolysis by

heterogeneous EF with an applied current density of 8.3 mA cm^{-2}. The excellent mineralization efficiency achieved without any initial pH adjustment was ascribed to heterogeneous EF reaction occurring on the surface of the $Fe^{II}Fe^{III}$-LDH catalyst, which catalyzed the decomposition of H_2O_2 to generate large amounts of hydroxyl radicals $^{\bullet}OH$ (Ganiyu et al., 2018). By comparison, only 59% removal of DOC was obtained in the reference experiment with analogous operating conditions but using raw CF as cathode instead of $Fe^{II}Fe^{III}$-LDH modified CF, thus highlighting the benefits obtained from the use of the modified cathode. Heterogeneous EF was also even more efficient than conventional homogeneous EF (90% removal of DOC after 8 h) with external addition of iron catalyst (0.2 mmol L^{-1}) and initial adjustment of pH at 3. Therefore, $Fe^{II}Fe^{III}$-LDH modified CF appeared as an ideal cathode material that enhances the mineralization efficiency of the EF process and avoids both initial pH adjustment and external addition of iron. The stability and reusability of the prepared $Fe^{II}Fe^{III}$-LDH modified CF cathode was assessed by reusing the same electrode for 4 successive electrolysis cycles (Fig. 2). The slight but continuous decrease of the efficiency could be ascribed to (i) the initial loss of loosely bounded $Fe^{II}Fe^{III}$-LDH at the external surface of the CF substrate due to vigorous stirring and/or (ii) iron leaching at acidic pH for which $Fe^{II}Fe^{III}$-LDH coating is less stable. Indeed, a progressive reduction of pH to values in the range 3 - 4 was noticed during electrolysis, which was explained by the generation of short-chain carboxylic acids. This leaching phenomenon was confirmed by comparison of SEM images of raw CF, $Fe^{II}Fe^{III}$-LDH modified CF before use and $Fe^{II}Fe^{III}$-LDH modified CF after 4 cycles of electrolysis (Fig. SI 2). While an extensive growth on the CF of dense platelets of $Fe^{II}Fe^{III}$-LDH with uneven and porous structure was initially obtained, a partial degradation of the global $Fe^{II}Fe^{III}$-LDH structure was observed after 4 cycles. Thus, in order to avoid the depletion of the catalyst, a continuous pH control

263 regulation would be recommended rather than a unique pH re-adjustment at the end of the
264 treatment.

265 Third, experiments were also performed at lower current density (4.2 mA cm^{-2}, Fig. 1B).
266 Lower DOC removal rates were obtained, e.g. 72% *vs* 96% removal of DOC after 8 h of
267 treatment by heterogeneous EF at 4.2 mA cm^{-2} and 8.3 mA cm^{-2}, respectively. Indeed, high
268 current density enhances the generation of hydrogen peroxide and regeneration rate of Fe(II).
269 Thus, further $^{\bullet}OH$ are produced for oxidation and mineralization of organic compounds.

270 Fourth, the influence of the anode material was also investigated (Fig. 1B). After 8h of
271 treatment by heterogeneous EF/AO using Ti_4O_7 anode at 4.2 mA cm^{-2}, 77% removal of DOC
272 was achieved, compared to 72% by heterogeneous EF using Pt anode. The higher efficiency
273 of Ti_4O_7 anode was ascribed to the generation at the anode surface of physisorbed $Ti_4O_7(^{\bullet}OH)$
274 with great oxidation ability, because of the higher overvoltage for oxygen evolution reaction
275 (>0.7 V), compared to Pt anode (<0.4 V) (Trellu et al., 2018a; Ganiyu et al., 2018). Therefore,
276 by taking also into consideration the lower cost of Ti_4O_7, this anode material appeared as a
277 suitable electrode to combine AO and EF processes.

278

279

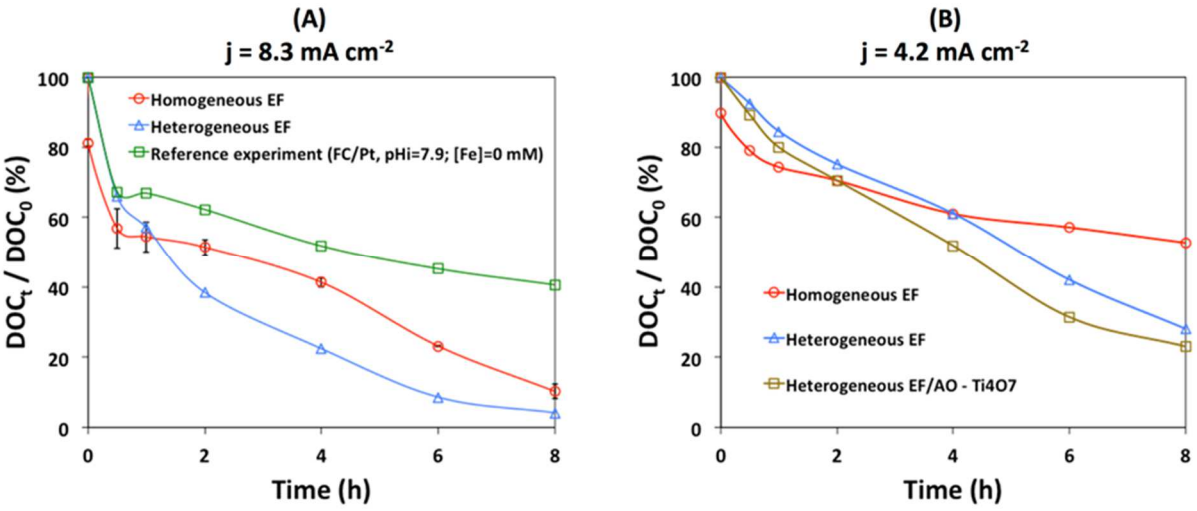

Figure 1 – DOC removal efficiency *vs* time during the mineralization of NF concentrate. Comparison of different configurations and operating conditions.

(A) j = 8.3 mA cm^{-2} : (○) Homogeneous EF with CF cathode, Pt anode, [Fe^{2+}] = 0.2 mmol L^{-1}, pH_0 = 3 ; (Δ) Heterogeneous EF with $Fe^{II}Fe^{III}$-LDH modified CF cathode, Pt anode, [Fe^{2+}] = 0 mmol L^{-1}, pH_0 = 7.9 ; (□) Reference experiment with CF cathode, Pt anode, [Fe^{2+}] = 0 mmol L^{-1}, pH_0 = 7.9. Three homogeneous EF experiments were performed in order to assess the reproducibility of the experimental procedure. Standard deviations are reported in Figure 1A.

(B) j = 4.2 mA cm^{-2} : (○) Homogeneous EF with CF cathode, Pt anode, [Fe^{2+}] = 0.2 mmol L^{-1}, pH_0 = 3 ; (Δ) Heterogeneous EF with $Fe^{II}Fe^{III}$-LDH modified CF cathode, Pt anode, [Fe^{2+}]= 0 mmol L^{-1}, pH_0 = 7.9 ; (□) Heterogeneous EF/AO with $Fe^{II}Fe^{III}$-LDH modified CF cathode, Ti_4O_7 anode, [Fe^{2+}] = 0 mmol L^{-1}, pH_0 = 7.9.

One of the main challenges for EAOPs is to reduce the energy consumption (EC). The EC was expressed as kWh per g of DOC removed and calculated from Eq. 6 (Brillas et al., 2009).

$$EC_{DOC}\ (\text{kWh}\ g^{-1}\ \text{of DOC}) = \frac{E_{cell} I t}{V \Delta(DOC)_{exp}} \qquad \text{(Eq. 6)}$$

where E_{cell} is the average cell voltage (V), I the applied current (A), t the duration of electrolysis (h), V the volume of solution treated (L) and $\Delta(DOC)_{exp}$ the experimental decays of DOC (mgC L^{-1}).

For example, 96% removal of DOC by heterogeneous EF at 8.3 mA cm^{-2} required 0.35 kWh g^{-1} of DOC removed. By comparison, 77% DOC removal by heterogeneous EF/AO using Ti_4O_7 anode at 4.2 mA cm^{-2} required only 0.13 kWh g^{-1} of DOC. This value decreased to 0.11 kWh g^{-1} of DOC for 45% removal of DOC by the same process (4 h of treatment instead of 8 h). In fact, high current density strongly increased energy consumption because of concomitant rise in total cell voltage (from 7.2 to 10.4 V). Parasitic reaction such as hydrogen evolution, 4 e^- reduction of O_2 to H_2O and 2 e^- oxidation of water to O_2 are also promoted at higher current density. Moreover, at high removal rate of DOC and low residual DOC, the current efficiency is strongly decreased by mass transport limitations. Therefore, in order to achieve high DOC removal rate with low energy consumption, it was proposed to combine EAOPs with a biological post-treatment, since EAOPs are able to transform biorefractory organic compounds into by-products that are more biodegradable than initial compounds (Ganzenko et al., 2014; Olvera-Vargas et al., 2015; Trellu et al., 2016a). In practice, that would mean implementing the EAOP as a preliminary treatment before recirculation of the NF concentrate towards the MBR. Thus, the next objective of this study was to monitor the evolution of the biodegradability of the effluent, as well as to better understand the evolution of organic and inorganic compounds during EAOPs.

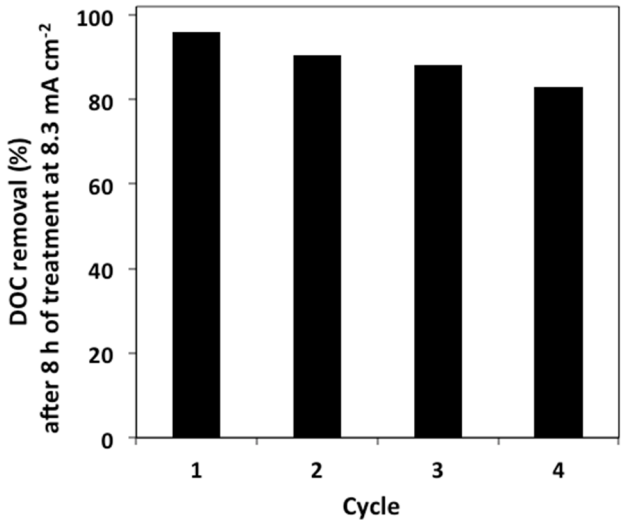

Figure 2 – DOC removal after 8h of electrolysis *vs* number of cycles for the heterogeneous EF treatment using $Fe^{II}Fe^{III}$-LDH/CF cathode and Pt anode at 8.3 mA cm^{-2}.

319

320

321 **3.3 Biodegradability enhancement**

322 Respirometric measurements performed have the advantage of being a direct and rapid
323 biological assessment of aerobic degradation under similar conditions than in the real
324 industrial MBR (Reuschenbach et al., 2003). The calculated biodegradability enhancement
325 (BE) values are presented in Fig. 3 after 4 and 8h of treatment for different EAOP
326 configurations and current densities applied.

327 In all cases, heterogeneous EF shows an increase in the biodegradability of the NF
328 concentrate, which validate the potenital positive role of EAOPs as a pre-treatment before
329 recirculating the NF concentrate to the MBR. In general the more the mineralization rate is
330 achieved the more the biodegradability enhancement is observed. After 8 h of treatment by
331 heterogeneous EF at 4.2 mA cm^{-2}, the BE index reached 11 with Ti_4O_7 anode, compared to
332 5.9 with Pt anode, which validate the positive effect of combining EF with AO. We could

state that a satisfactory biodegradability enhancement (between 4.1 and 9.1) was reached after 4 h with optimal energy consumption efficiency.

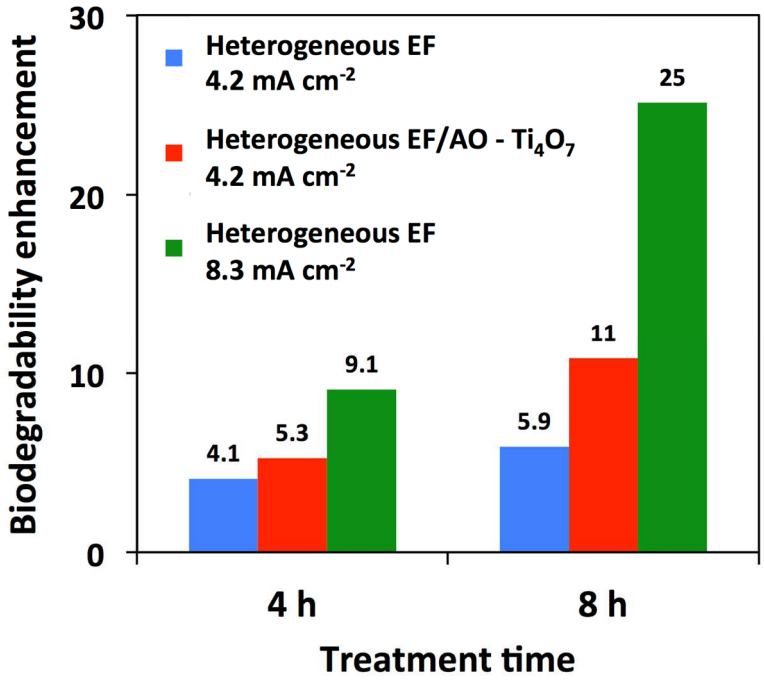

Figure 3 – Biodegradability enhancement at two different treatment times for different EAOPs and current densities.

3.4 Acute toxicity of the effluent

Toxicity evolution of the NF concentrate during its electrolysis by both heterogeneous and homogeneous EF was evaluated by Microtox® standard method (Fig. 4). Initially (i.e. before any treatment of the NF concentrate), around 50±5% of *V. fischeri* luminescence inhibition was observed because of the presence of large amount of toxic trace metals and organic pollutants. *V. fischeri* luminescence inhibition can be sensitive to various phenomena that can not be controlled and studied separately during the treatment of such complex effluent, e.g. the removal of toxic organic pollutants, the formation of toxic degradation by-products, the

formation of non-toxic degradation by-products (which could promote stimulation of bacterial luminescence), the release of inorganic compounds and the evolution of metal speciation. Therefore, it is difficult to draw reliable conclusions from these analyses. However, results show that EAOPs are not able to remove completely the acute toxicity from such complex effluent containing both organic and inorganic toxic compounds. Luminescence inhibtion might even increases significantly, particularly after achieving high mineralization rates (for example during heterogeneous EF at 8.3 mA cm^{-2} and heterogeneous EF at 4.2 mA cm^{-2}). From the comparison of heterogeneous EF experiments performed with either Pt or Ti_4O_7 anode, it seems that anodic oxidation participate to avoid the accumulation of toxic by-products in the bulk.

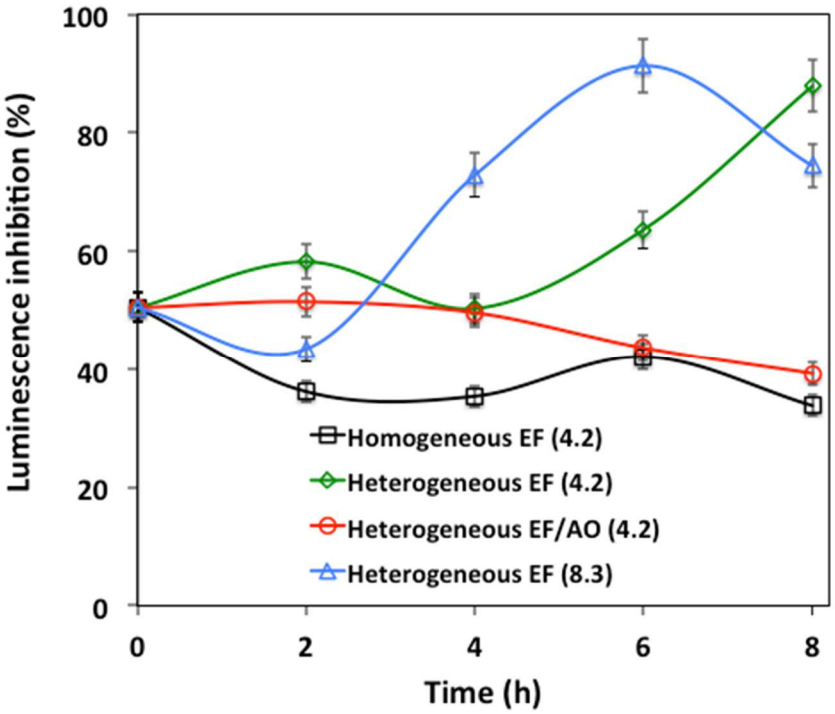

Figure 4 – Evolution of *Vibrio fisheri* luminescence inhibition (Microtox® test) *vs* electrolysis time according to EAOP configuration and current density (in brackets, mA cm^{-2})

3.5 Characterization of the organic matter by 3DEEM

3DEEM has been reported to be a useful tool for characterization of colloidal and dissolved organic matter. Particularly, Jacquin et al. (2017) recently emphasized a correlation between the volume of fluorescence of zone III' (HA+FA-like fluorophores) and the concentration in a full-scale MBR of humic substances (MW ≈ 1000 Da) and building blocks (degradation by-products from humic substances, with MW ≈ 300-500 Da) measured by size exclusion liquid chromatography coupled with organic carbon and organic nitrogen detector. Similarly, a correlation was also obtained between the volume of fluorescence of zone II' (SMP-like fluorophores) and the concentration of proteins from biopolymers (MW ≈ 20,000 - 7.5 x 10^{11} Da). Besides, no correlation was obtained for the volume of fluorescence of zone I' because fluorophores of this zone would be mostly associated with colloidal proteins that could not be analyzed by size exclusion liquid chromatography (Jacquin et al., 2017). In this study, we proposed to use these results with the view to obtain indications on the evolution of the nature of the organic matter during EAOPs.

The initial effluent was mainly constituted of HA+FA-like fluorophores from zone III' as shown in Fig. 5A and 5B. This result is consistent with the pre-treatment of the effluent in the MBR because microfiltration membranes have lower retention capacity for these low MW compounds. A strong decrease of fluorophores of zone III' was then observed during both heterogeneous EF (Fig. 5C) and EF/AO (Fig. 5D) due to (i) precipitation of humic acids at acidic pH and (ii) fast degradation and mineralization of these low MW compounds with an aromatic structure that reacts quickly with $^{\bullet}OH$ (Trellu et al., 2016b). By comparison, fluorescence from colloidal proteins of zone I' decreased much more slowly. This phenomenon might be ascribed to the lower availability of colloids for reaction with $^{\bullet}OH$ in the aqueous phase. In the context of the global combined process, this result means that improving the retention of colloidal proteins in the MBR would then have a positive effect on

384 the efficiency of the EAOP. Finally, it was also observed that the use of Ti_4O_7 anode for the
385 heterogeneous AO/EF process promoted significantly the decrease of the fluorescence of
386 proteins from biopolymers (zone II', Fig. 5D). This might be ascribed to the higher electro-
387 catalytic activity of Ti_4O_7 for anodic oxidation of organic compounds, compared to Pt anode
388 (Ganiyu et al., 2016).

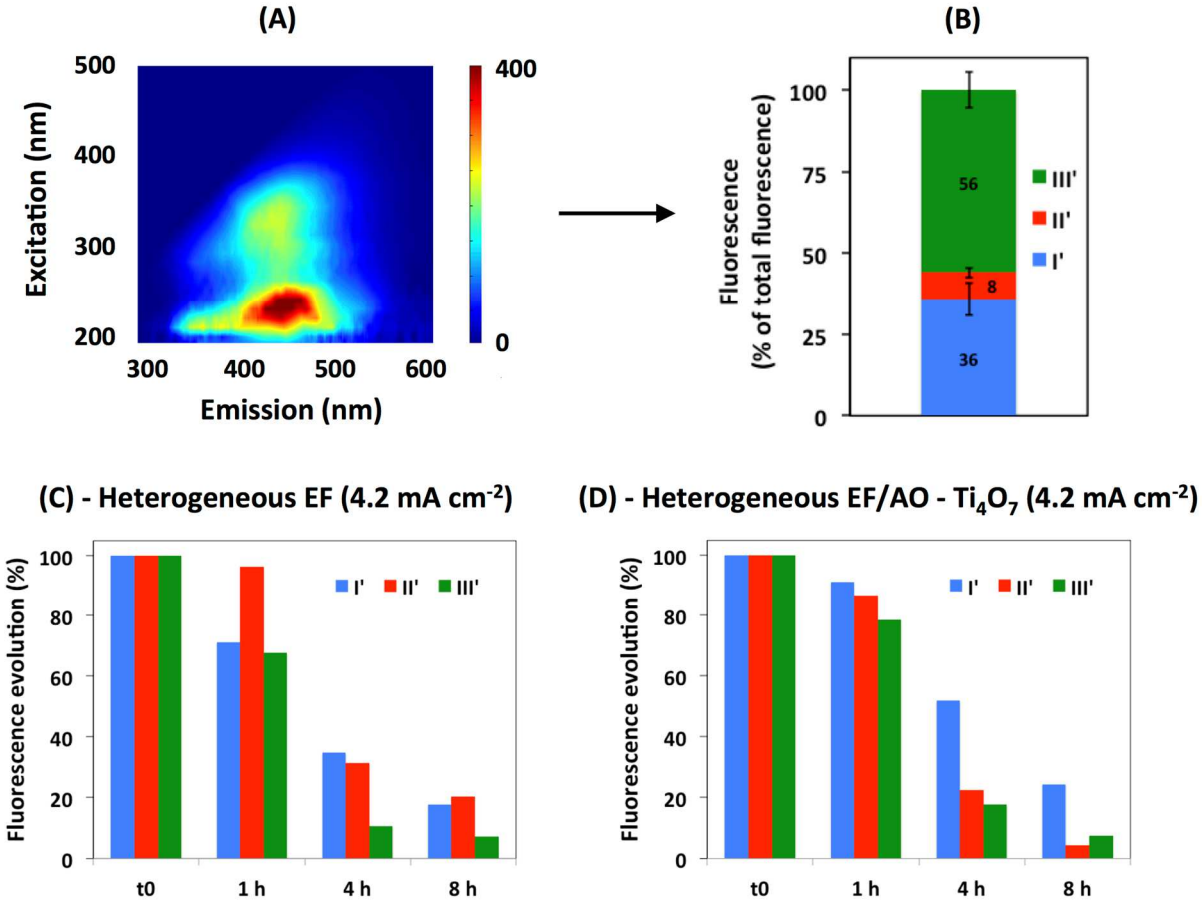

389

390 **Figure 5** – Fluorescence evolution of the NF concentrate effluent treated by EAOPs, as a
391 function of time treatment. Zone I': colloidal proteins ; zone II': Soluble Microbial by-
392 Product (SMP)-like fluorophores ; zone III': Humic and Fulvic acids (HA + FA)-like
393 fluorophores.

394

395

3.6 Identification and quantification of short-chain carboxylic acids

Short-chain carboxylic acids are common degradation by-products generated during the degradation of organic compounds by EAOPs (Oturan et al., 2008). In this study, they were identified by ion-exclusion HPLC and chromatograms revealed five well defined peaks corresponding to acetic, formic, succinic, malonic and oxamic acids. Results were firstly analyzed by following the evolution of the concentration of the sum of carboxylic acids analyzed. The evolution of the concentration according to treatment time was determined for homogeneous EF at 8.3 mA cm^{-2}. An initial increase of the concentration was observed until t = 6 h ([Σ carboxylic acids] = 55 mgC L^{-1}) because of the degradation of aromatic pollutants. Then, the concentration decreased ([Σ carboxylic acids] = 34 mgC L^{-1} at t = 8 h). In fact, the lower concentration of organic compounds after 6 hours of treatment resulted in lower formation rate of carboxylic acids compared to the degradation rate. Interestingly, Fig. 6A shows a linear correlation (R^2 = 0.92) between DOC removal (%) and proportion of carboxylic acids among the residual DOC. This correlation took into consideration all analyzes performed for the different configurations tested. The higher the DOC removal achieved, the higher was the proportion of carboxylic acids among the residual DOC. This result is consistent with the lower reaction rate constant of short-chain carboxylic acids with $^{\bullet}OH$ (10^7 - 10^8 M^{-1} s^{-1}) compared to aromatic compounds (10^9 - 10^{10} M^{-1} s^{-1}) from which they are formed (Oturan et al., 2008). The evolution of the proportion of each single carboxylic acid was also studied (Fig. 6B). It was noticed that the proportion of acetic acid among total carboxylic acid concentration was continuously increased over time during homogeneous EF at 8.3 mA cm^{-2}. This phenomenon is also consistent with the lower reaction rate constant of acetic acid with $^{\bullet}OH$ (1.6 x 10^7 M^{-1} s^{-1}) compared to other carboxylic acids (Oturan et al., 2008). Similar trend was observed after 8 h of electrolysis using heterogeneous EF at 8.3 mA cm^{-2} or 4.2 mA cm^{-2} and homogeneous EF at 4.2 mA cm^{-2}, i.e. the higher the DOC removal

rate (Fig. 1), the higher the proportion of acetic acid. Heterogeneous EF/AO using Ti_4O_7 was the only experiment exhibiting a different trend, thus indicating that Ti_4O_7 might modify mineralization mechanisms, compared to Pt anode. Higher proportion of N-containing oxamic acid and lower proportion of acetic acid were observed with Ti_4O_7 anode, which might be attributed to the better electro-catalytic ability of Ti_4O_7 anode for the degradation of organic nitrogen and acetic acid, compared to Pt anode. As regards to oxamic acid, these results were consistent with 3DEEM. In fact, Ti_4O_7 anode further degraded proteins from biopolymers (zone II'), which usually contain high concentration of N (ratio C/N around 3) (Jacquin et al., 2017). Overall, the increase of the proportion of carboxylic acids over time confirms the suitability of the combination of EAOPs with a biological treatment (Fig. 3), because of the well-known high biodegradability of such compounds.

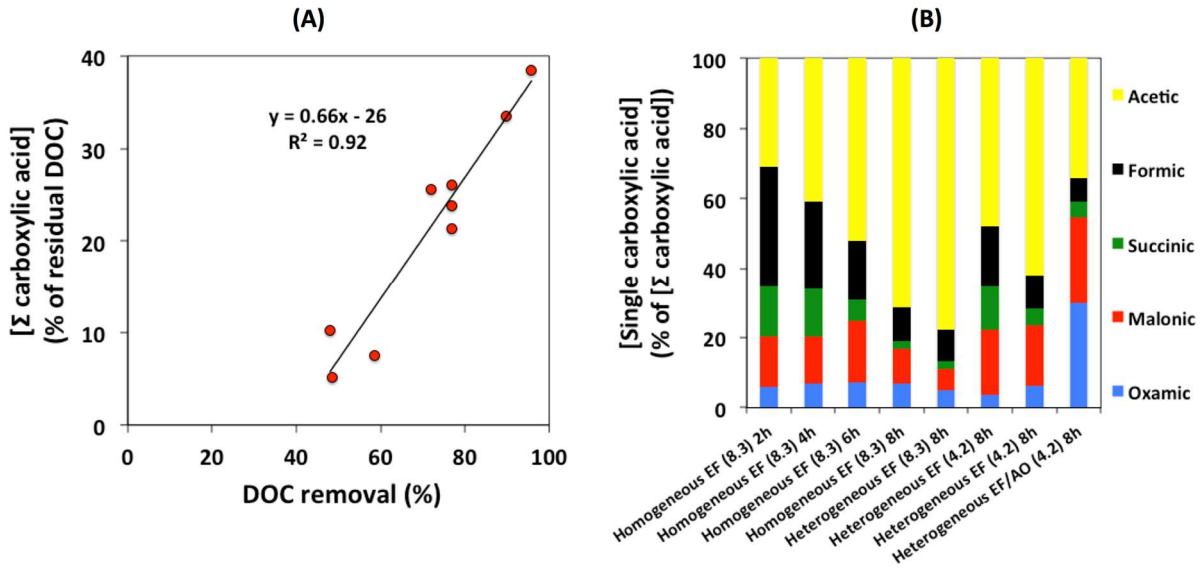

Figure 6 – Generation of short-chain carboxylic acids during EAOPs: (A) correlation between DOC removal (%) and proportion of carboxylic acids among the residual DOC; (B) evolution of the proportion of each single carboxylic acid among the total carboxylic acid concentration as a function of configurations and operating conditions (current density in bracket, mA cm^{-2}).

3.7 Evolution of inorganic species

Mineralization of Cl^- and N-containing organic compounds was accompanied by the formation of inorganic ions. The main inorganic species of interest (NO_3^-, NH_4^+, ClO_3^- and ClO_4^-) were analyzed by ion chromatography. Results are presented in Fig. 7. In all experiments, a stronger increase of the concentration of NH_4^+ was observed compared to NO_3^- (Fig. 7A and 7B). These results can be explained by (i) the direct release of NH_4^+ from mineralization of organic nitrogen and (ii) the release of NO_3^- followed by reduction of NO_3^- into NH_4^+ at the cathode. Actually, the latter reaction is often observed during EF and AO, while oxidation of NH_4^+ at the anode is hindered by the positive charge of this ion (Martin de Vidales et al., 2016; Mousset et al., 2018). The amount of NH_4^+ in the solution increased with treatment time and current density because of the higher mineralization rate of organic nitrogen (Fig. 7B). Higher concentration of NH_4^+ was also obtained using Ti_4O_7 anode (heterogeneous EF/AO), compared to Pt anode (heterogeneous EF). This phenomenon is consistent with the results obtained from 3DEEM and with the higher concentration of oxamic acid previously reported, and supports the higher electro-catalytic activity of Ti_4O_7 for the degradation of organic nitrogen. In the context of a treatment strategy including a recirculation of the effluent back to the MBR, the release of NH_4^+ during EAOPs would require further biological nitrification in the MBR.

Oxidation of Cl^- resulted in a strong increase of ClO_3^- concentration (Fig. 7C). The reaction mechanisms usually go through Cl^- oxidation into Cl_2, followed by hydrolysis of Cl_2 into hypochlorous acid HOCl. Further oxidation of HOCl lead to the formation of ClO_2^- (which was not detected because of the fast oxidation kinetic) and subsequently ClO_3^-. No formation of ClO_4^- was detected in any experiment because higher current density (> 30 mA cm^{-2}) is required to form this compound (Mousset et al., 2018). Besides, it was also observed that the formation of ClO_3^- mainly occurred between 4 and 8 h of treatment, most probably because of

463 the preferential reaction of HOCl with organic species and NH_4^+ (break-point chlorination)
464 between 4 and 8 h of treatment (Martin de Vidales et al., 2016; Mousset et al., 2018). These
465 results confirm the suitability to stop the treatment after 4 h of treatment in order to avoid the
466 accumulation of ClO_3^- and NH_4^+. While ClO_3^- can be toxic for the biomass in the MBR, the
467 formation of NH_3 at basic pH is also highly toxic for the autotrophic biomass (Jacquin et al.,
468 2018).

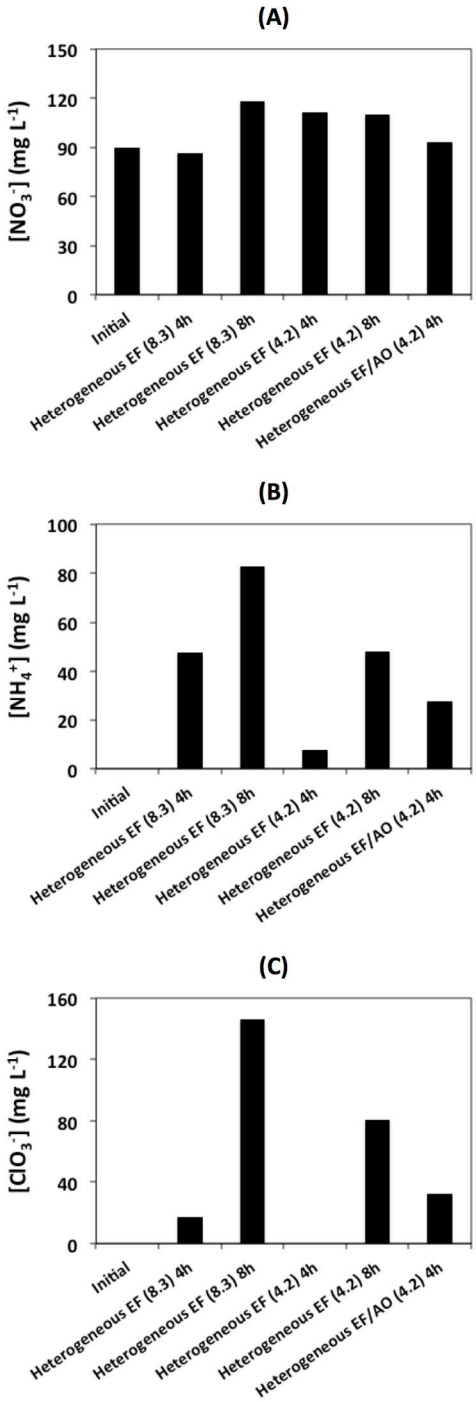

469 **Figure 7** – Concentration evolution of main inorganic species of interest during EAOPs as a
470 function of configurations and operating conditions (current density in bracket, mA cm^{-2}): (A)
471 ClO_3^-, (B) NO_3^- and (C) NH_4^+. ClO_4^- was not detected.

472

473

4. Conclusion

NF concentrate of landfill leachate pre-treated in a MBR contains high concentration of biorefractory organic pollutants that makes very difficult to treat or detoxify by conventional techniques. The investigation of different configurations of EAOPs applied to this complex effluent showed that heterogeneous EF/AO using Ti_4O_7 anode and $Fe^{II}Fe^{III}$-LDH modified CF cathode is the most efficient process for mineralization of organic pollutants. Without initial pH adjustment and external addition of Fe^{2+} in the bulk, 45% removal of DOC was achieved at 4.2 mA cm^{-2} with limited energy consumption (0.11 kWh g^{-1} of DOC removed, i.e. 49.5 kWh m^{-3}). Up to 96% removal of DOC was also obtained by using higher current density (8.3 mA cm^{-2}) during the heterogeneous EF process. The use of Ti_4O_7 anode appeared to be a key parameter for improving the degradation and mineralization of organic nitrogen. From 3DEEM analysis, colloidal proteins were observed to be the most refractory organic compounds. Therefore, improving the retention of such compounds in the MBR could improve the efficiency of the EAOP.

The acute toxicity of the effluent was not removed but strong biodegradability enhancement was observed after 4 h of treatment by heterogeneous EF/AO, thus making possible the recirculation of the residual DOC towards the MBR in order to achieve total COD removal without longer electrochemical treatment time. This result was consistent with the identification and quantification of more biodegradable and less toxic by-products such as carboxylic acids. In fact, a linear correlation was observed between DOC removal rate and proportion of carboxylic acids in the residual DOC. As regards to the fate of inorganic species, the formation of ClO_3^- could be limited by stopping electro-oxidation at 4 h, but enhanced nitrification would be required in the MBR because of the release of NH_4^+ from mineralization of organic nitrogen. Overall, these results emphasized the interdependence

between the MBR process and the EAOP in a combined treatment strategy and demonstrated that the use of EAOPs using suitable electrode materials can be useful for the management of such complex effluent.

Acknowledgements

We gratefully acknowledge the National French Agency of Research 'ANR' for funding the project ECOTS/CELECTRON. Authors are also grateful to Saint Gobain Research Provence for supplying Ti_4O_7 electrodes.

References

Amaral, M.C., Moravia, W.G., Lange, L.C., Zico, M.R., Magalhães, N.C., Ricci, B.C., Reis, B.G., 2016. Pilot aerobic membrane bioreactor and nanofiltration for municipal landfill leachate treatment. Journal of Environmental Science and Health, Part A 51, 640–649.

Ammar, S., Oturan, M.A., Labiadh, L., Guersalli, A., Abdelhedi, R., Oturan, N., Brillas, E., 2015. Degradation of tyrosol by a novel electro-Fenton process using pyrite as heterogeneous source of iron catalyst. Water Research 74, 77–87. https://doi.org/10.1016/j.watres.2015.02.006

Brillas, E., Sirés, I., Oturan, M.A., 2009. Electro-Fenton Process and Related Electrochemical Technologies Based on Fenton's Reaction Chemistry. Chemical Reviews 109, 6570–6631. https://doi.org/10.1021/cr900136g

Campagna, M., Çakmakcı, M., Büşra Yaman, F., Özkaya, B., 2013. Molecular weight distribution of a full-scale landfill leachate treatment by membrane bioreactor and nanofiltration membrane. Waste Management 33, 866–870. https://doi.org/10.1016/j.wasman.2012.12.010

Chen, W., Westerhoff, P., Leenheer, J.A., Booksh, K., 2003. Fluorescence Excitation−Emission Matrix Regional Integration to Quantify Spectra for Dissolved Organic Matter. Environmental Science & Technology 37, 5701–5710. https://doi.org/10.1021/es034354c

Comninellis, C., Kapalka, A., Malato, S., Parsons, S.A., Poulios, I., Mantzavinos, D., 2008. Advanced oxidation processes for water treatment: Advances and trends for R&D. J. Chem. Technol. Biotechnol. 83, 769–776. https://doi.org/10.1002/jctb.1873

Cui, Y.-H., Xue, W.-J., Yang, S.-Q., Tu, J.-L., Guo, X.-L., Liu, Z.-Q., 2018. Electrochemical/peroxydisulfate/Fe3+ treatment of landfill leachate nanofiltration concentrate after ultrafiltration. Chemical Engineering Journal 353, 208–217. https://doi.org/10.1016/j.cej.2018.07.101

Ganiyu, S.O., Huong Le, T.X., Bechelany, M., Oturan, N., Papirio, S., Esposito, G., van Hullebusch, E., Cretin, M., Oturan, M.A., 2018. Electrochemical mineralization of sulfamethoxazole over wide pH range using FeIIFeIII LDH modified carbon felt cathode: Degradation pathway, toxicity and reusability of the modified cathode. Chemical Engineering Journal 350, 844–855. https://doi.org/10.1016/j.cej.2018.04.141

Ganiyu, S.O., Le, T.X.H., Bechelany, M., Esposito, G., Hullebusch, E.D. van, Oturan, M.A., Cretin, M., 2017a. A hierarchical CoFe-layered double hydroxide modified carbon-felt cathode for heterogeneous electro-Fenton process. J. Mater. Chem. A 5, 3655–3666. https://doi.org/10.1039/C6TA09100H

Ganiyu, S.O., Oturan, N., Raffy, S., Cretin, M., Esmilaire, R., van Hullebusch, E., Esposito, G., Oturan, M.A., 2016. Sub-stoichiometric titanium oxide (Ti4O7) as a suitable ceramic anode for electrooxidation of organic pollutants: A case study of kinetics, mineralization and

552 toxicity assessment of amoxicillin. Water Research 106, 171–182.
553 https://doi.org/10.1016/j.watres.2016.09.056

554 Ganiyu, S.O., Oturan, N., Raffy, S., Esposito, G., van Hullebusch, E.D., Cretin, M., Oturan,
555 M.A., 2017b. Use of Sub-stoichiometric Titanium Oxide as a Ceramic Electrode in Anodic
556 Oxidation and Electro-Fenton Degradation of the Beta-blocker Propranolol: Degradation
557 Kinetics and Mineralization Pathway. Electrochimica Acta 242, 344–354.
558 https://doi.org/10.1016/j.electacta.2017.05.047

559 Ganiyu, S. O., Zhou, M., Martínez-Huitle, C. A., 2018. Heterogeneous electro-Fenton and
560 photoelectro-Fenton processes: a critical review of fundamental principles and application
561 for water/wastewater treatment. Applied Catalysis B: Environmental 235, 103-129.
562 https://doi.org/10.1016/j.apcatb.2018.04.044

563 Ganzenko, O., Huguenot, D., van Hullebusch, E.D., Esposito, G., Oturan, M.A., 2014.
564 Electrochemical advanced oxidation and biological processes for wastewater treatment: a
565 review of the combined approaches. Environmental Science and Pollution Research 21,
566 8493–8524. https://doi.org/10.1007/s11356-014-2770-6

567 Ganzenko, O., Trellu, C., Papirio, S., Oturan, N., Huguenot, D., van Hullebusch, E.D., Esposito,
568 G., Oturan, M.A., 2018. Bioelectro-Fenton: evaluation of a combined biological—advanced
569 oxidation treatment for pharmaceutical wastewater. Environmental Science and Pollution
570 Research 25, 20283–20292. https://doi.org/10.1007/s11356-017-8450-6

571 García-Rodríguez, O., Bañuelos, J.A., El-Ghenymy, A., Godínez, L.A., Brillas, E., Rodríguez-
572 Valadez, F.J., 2016. Use of a carbon felt–iron oxide air-diffusion cathode for the
573 mineralization of Malachite Green dye by heterogeneous electro-Fenton and UVA
574 photoelectro-Fenton processes. Journal of Electroanalytical Chemistry 767, 40–48.
575 https://doi.org/10.1016/j.jelechem.2016.01.035

576 Guo, L., Jing, Y., Chaplin, B.P., 2016. Development and Characterization of Ultrafiltration TiO2
577 Magnéli Phase Reactive Electrochemical Membranes. Environ. Sci. Technol. 50, 1428–1436.
578 https://doi.org/10.1021/acs.est.5b04366

579 Hu, Y., Lu, Y., Liu, G., Luo, H., Zhang, R., Cai, X., 2018. Effect of the structure of stacked
580 electro-Fenton reactor on treating nanofiltration concentrate of landfill leachate.
581 Chemosphere 202, 191–197. https://doi.org/10.1016/j.chemosphere.2018.03.103

582 Iglesias, O., Fernández de Dios, M.A., Pazos, M., Sanromán, M.A., 2013. Using iron-loaded
583 sepiolite obtained by adsorption as a catalyst in the electro-Fenton oxidation of Reactive
584 Black 5. Environmental Science and Pollution Research 20, 5983–5993.
585 https://doi.org/10.1007/s11356-013-1610-4

586 Jacquin, C., Lesage, G., Traber, J., Pronk, W., Heran, M., 2017. Three-dimensional excitation
587 and emission matrix fluorescence (3DEEM) for quick and pseudo-quantitative determination
588 of protein- and humic-like substances in full-scale membrane bioreactor (MBR). Water
589 Research 118, 82–92. https://doi.org/10.1016/j.watres.2017.04.009

590 Jacquin, C., Monnot, M., Hamza, R., Kouadio, Y., Zaviska, F., Merle, T., Lesage, G., Héran, M.,

591 2018. Link between dissolved organic matter transformation and process performance in a
592 membrane bioreactor for urinary nitrogen stabilization. Environmental Science: Water
593 Research & Technology 4, 806–819. https://doi.org/10.1039/C8EW00029H

594 Kjeldsen, P., Barlaz, M.A., Rooker, A.P., Baun, A., Ledin, A., Christensen, T.H., 2002. Present
595 and Long-Term Composition of MSW Landfill Leachate: A Review. Critical Reviews in
596 Environmental Science and Technology 32, 297–336.
597 https://doi.org/10.1080/10643380290813462

598 Li, X., Zhu, W., Wu, Y., Wang, C., Zheng, J., Xu, K., Li, J., 2015. Recovery of potassium from
599 landfill leachate concentrates using a combination of cation-exchange membrane
600 electrolysis and magnesium potassium phosphate crystallization. Separation and Purification
601 Technology 144, 1–7. https://doi.org/10.1016/j.seppur.2015.01.035

602 Ma, L., Zhou, M., Ren, G., Yang, W., Liang, L., 2016. A highly energy-efficient flow-through
603 electro-Fenton process for organic pollutants degradation. Electrochimica Acta 200, 222–
604 230. https://doi.org/10.1016/j.electacta.2016.03.181

605 Mahindrakar, K.V., Rathod, V.K., 2018. Utilization of banana peels for removal of strontium
606 (II) from water. Environmental Technology & Innovation 11, 371–383.
607 https://doi.org/10.1016/j.eti.2018.06.015

608 Martin de Vidales, M.J., Millán, M., Sáez, C., Cañizares, P., Rodrigo, M.A., 2016. What
609 happens to inorganic nitrogen species during conductive diamond electrochemical oxidation
610 of real wastewater? Electrochemistry Communications 67, 65–68.
611 https://doi.org/10.1016/j.elecom.2016.03.014

612 Martínez-Huitle, C.A., Rodrigo, M.A., Sirés, I., Scialdone, O., 2015. Single and Coupled
613 Electrochemical Processes and Reactors for the Abatement of Organic Water Pollutants: A
614 Critical Review. Chem. Rev. 115, 13362–13407.
615 https://doi.org/10.1021/acs.chemrev.5b00361

616 Mousset, E., Pontvianne, S., Pons, M.-N., 2018. Fate of inorganic nitrogen species under
617 homogeneous Fenton combined with electro-oxidation/reduction treatments in synthetic
618 solutions and reclaimed municipal wastewater. Chemosphere 201, 6–12.
619 https://doi.org/10.1016/j.chemosphere.2018.02.142

620 Oller, I., Malato, S., Sánchez-Pérez, J.A., 2011. Combination of Advanced Oxidation Processes
621 and biological treatments for wastewater decontamination—A review. Science of The Total
622 Environment 409, 4141–4166. https://doi.org/10.1016/j.scitotenv.2010.08.061

623 Olvera-Vargas, H., Cocerva, T., Oturan, N., Buisson, D., Oturan, M.A., 2015. Bioelectro-
624 Fenton: A sustainable integrated process for removal of organic pollutants from water:
625 Application to mineralization of metoprolol. J. Hazard. Mater.
626 https://doi.org/10.1016/j.jhazmat.2015.12.010

627 Oturan, M.A., Pimentel, M., Oturan, N., Sirés, I., 2008. Reaction sequence for the
628 mineralization of the short-chain carboxylic acids usually formed upon cleavage of aromatics
629 during electrochemical Fenton treatment. Electrochimica Acta 54, 173–182.

https://doi.org/10.1016/j.electacta.2008.08.012

Oturan, N., van Hullebusch, E.D., Zhang, H., Mazeas, L., Budzinski, H., Le Menach, K., Oturan, M.A., 2015. Occurrence and Removal of Organic Micropollutants in Landfill Leachates Treated by Electrochemical Advanced Oxidation Processes. Environmental Science & Technology 49, 12187–12196. https://doi.org/10.1021/acs.est.5b02809

Özcan, A., Sahin, Y., Koparal, A.S., Oturan, M.A., 2008. Propham mineralization in aqueous medium by anodic oxidation using boron-doped diamond anode: Influence of experimental parameters on degradation kinetics and mineralization efficiency. Water Res. 42, 2889–2898. https://doi.org/10.1016/j.watres.2008.02.027

Panizza, M., Cerisola, G., 2009. Direct and mediated anodic oxidation of organic pollutants. Chem. Rev. 109, 6541–6569. https://doi.org/10.1021/cr9001319

Ponthieu, M., Pinel-Raffaitin, P., Le Hecho, I., Mazeas, L., Amouroux, D., Donard, O.F.X., Potin-Gautier, M., 2007. Speciation analysis of arsenic in landfill leachate. Water Research 41, 3177–3185. https://doi.org/10.1016/j.watres.2007.04.026

Poza-Nogueiras, V., Rosales, E., Pazos, M., Sanromán, M. Á. (2018). Current advances and trends in electro-Fenton process using heterogeneous catalysts–a review. Chemosphere 201, 399-416. https://doi.org/10.1016/j.chemosphere.2018.03.002

Radjenovic, J., Sedlak, D.L., 2015. Challenges and Opportunities for Electrochemical Processes as Next-Generation Technologies for the Treatment of Contaminated Water. Environ. Sci. Technol. 49, 11292–11302. https://doi.org/10.1021/acs.est.5b02414

Reuschenbach, P., Pagga, U., Strotmann, U., 2003. A critical comparison of respirometric biodegradation tests based on OECD 301 and related test methods. Water Research 37, 1571–1582. https://doi.org/10.1016/S0043-1354(02)00528-6

Sirés, I., Brillas, E., Oturan, M.A., Rodrigo, M.A., Panizza, M., 2014. Electrochemical advanced oxidation processes: today and tomorrow. A review. Environ Sci Pollut Res 21, 8336–8367. https://doi.org/10.1007/s11356-014-2783-1

Trellu, C., Chaplin, B.P., Coetsier, C., Esmilaire, R., Cerneaux, S., Causserand, C., Cretin, M., 2018a. Electro-oxidation of organic pollutants by reactive electrochemical membranes. Chemosphere 208, 159–175. https://doi.org/10.1016/j.chemosphere.2018.05.026

Trellu, C., Coetsier, C., Rouch, J.-C., Esmilaire, R., Rivallin, M., Cretin, M., Causserand, C., 2018b. Mineralization of organic pollutants by anodic oxidation using reactive electrochemical membrane synthesized from carbothermal reduction of TiO2. Water Research 131, 310–319. https://doi.org/10.1016/j.watres.2017.12.070

Trellu, C., Ganzenko, O., Papirio, S., Pechaud, Y., Oturan, N., Huguenot, D., van Hullebusch, E.D., Esposito, G., Oturan, M.A., 2016a. Combination of anodic oxidation and biological treatment for the removal of phenanthrene and Tween 80 from soil washing solution. Chemical Engineering Journal 306, 588–596. https://doi.org/10.1016/j.cej.2016.07.108

Trellu, C., Oturan, N., Pechaud, Y., van Hullebusch, E.D., Esposito, G., Oturan, M.A., 2017.

668 Anodic oxidation of surfactants and organic compounds entrapped in micelles – Selective
669 degradation mechanisms and soil washing solution reuse. Water Research 118, 1–11.
670 https://doi.org/10.1016/j.watres.2017.04.013

671 Trellu, C., Péchaud, Y., Oturan, N., Mousset, E., Huguenot, D., van Hullebusch, E.D., Esposito,
672 G., Oturan, M.A., 2016b. Comparative study on the removal of humic acids from drinking
673 water by anodic oxidation and electro-Fenton processes: Mineralization efficiency and
674 modelling. Applied Catalysis B: Environmental 194, 32–41.
675 https://doi.org/10.1016/j.apcatb.2016.04.039

676 Van der Bruggen, B., Koninckx, A., Vandecasteele, C., 2004. Separation of monovalent and
677 divalent ions from aqueous solution by electrodialysis and nanofiltration. Water Research
678 38, 1347–1353. https://doi.org/10.1016/j.watres.2003.11.008

679 Van der Bruggen, B., Lejon, L., Vandecasteele, C., 2003. Reuse, Treatment, and Discharge of
680 the Concentrate of Pressure-Driven Membrane Processes. Environmental Science &
681 Technology 37, 3733–3738. https://doi.org/10.1021/es0201754

682 Wang, Yujing, Zhao, G., Chai, S., Zhao, H., Wang, Yanbin, 2013. Three-Dimensional
683 Homogeneous Ferrite-Carbon Aerogel: One Pot Fabrication and Enhanced Electro-Fenton
684 Reactivity. ACS Applied Materials & Interfaces 5, 842–852.
685 https://doi.org/10.1021/am302437a

686 Westerhoff, P., Prapaipong, P., Shock, E., Hillaireau, A., 2008. Antimony leaching from
687 polyethylene terephthalate (PET) plastic used for bottled drinking water. Water Research 42,
688 551–556. https://doi.org/10.1016/j.watres.2007.07.048

689 Xu, Y., Chen, C., Li, X., Lin, J., Liao, Y., Jin, Z., 2017. Recovery of humic substances from
690 leachate nanofiltration concentrate by a two-stage process of tight ultrafiltration membrane.
691 Journal of Cleaner Production 161, 84–94. https://doi.org/10.1016/j.jclepro.2017.05.095

692 Zhang, G., Wang, S., Yang, F., 2012. Efficient Adsorption and Combined
693 Heterogeneous/Homogeneous Fenton Oxidation of Amaranth Using Supported Nano-FeOOH
694 As Cathodic Catalysts. The Journal of Physical Chemistry C 116, 3623–3634.
695 https://doi.org/10.1021/jp210167b

696 Zhang, H., Fei, C., Zhang, D., Tang, F., 2007. Degradation of 4-nitrophenol in aqueous
697 medium by electro-Fenton method. Journal of Hazardous Materials 145, 227–232.
698 https://doi.org/10.1016/j.jhazmat.2006.11.016

699 Zhang, L., Li, A., Lu, Y., Yan, L., Zhong, S., Deng, C., 2009. Characterization and removal of
700 dissolved organic matter (DOM) from landfill leachate rejected by nanofiltration. Waste
701 Management 29, 1035–1040. https://doi.org/10.1016/j.wasman.2008.08.020

702 Zhang, Q.-Q., Tian, B.-H., Zhang, X., Ghulam, A., Fang, C.-R., He, R., 2013. Investigation on
703 characteristics of leachate and concentrated leachate in three landfill leachate treatment
704 plants. Waste Management 33, 2277–2286. https://doi.org/10.1016/j.wasman.2013.07.021